9

BEYOND HODGKIN AND HUXLEY: CALCIUM AND CALCIUM-DEPENDENT POTASSIUM CURRENTS

The cornerstone of modern biophysics is the comprehensive analysis by Hodgkin and Huxley (1952a,b,c,d) of the generation and propagation of action potentials in the squid giant axon. The basis of their model is a fast sodium current I_{Na} and a delayed potassium current I_K (which here we also refer to as I_{DR}). The last 40 years of research have shown that impulse conduction along axons can be successfully analyzed in terms of one or both of these currents (see Sec. 6.6). Nonetheless, their equations do not capture—nor were they intended to capture—a number of important biophysical phenomena, such as adaptation of the firing frequency to long-lasting stimuli or bursting, that is, the generation of two to five spikes within 5–20 msec. Moreover, the transmission of electrical signals within and between neurons involves more than the mere circulation of stereotyped pulses. These impulses must be set up and generated by subthreshold processes.

The differences between the firing behavior of most neurons and the squid giant axon reflect the roles of other voltage-dependent ionic conductances than the two described by Hodgkin and Huxley. Over the last two decades, more than several dozen membrane conductances have been characterized (Hagiwara, 1983; Llinás, 1988; Hille, 1992). They differ in principal carrier, voltage, and time dependence, dependence on the presence of intracellular calcium and on their susceptibility to modulation by synaptic inputs and second messengers. Our knowledge of these conductances and the role they play in impulse formation has accelerated rapidly in recent years as a result of various technical innovations such as single-cell isolation, patch clamping, and molecular techniques. We will here describe the most important of these conductances and briefly characterize each one. In order to understand more completely the functional role of these conductances in determining the response of the cell to input, empirical equations that approximate their behavior under physiological conditions must be developed and compared against the physiological preparations. In a remarkable testimony to the power and the generality

of the Hodgkin–Huxley approach, the majority of such phenomenological models has used their methodology of describing individual ionic conductances in terms of activating and inactivating particles with first-order kinetics (see Chap. 6). Theirs is also our method of choice for quantifying the membrane conductance that we use throughout this book.

Because of the large number of ionic conductances that have been described throughout the nervous systems of different animals, we would certainly exhaust the patience of the reader by listing and describing them all (as Llinás, 1988, has done). Instead, we focus on a few key conductances, in particular those that appear to be common to many neurons in most animals, from slugs and flies to mammals.

9.1 Calcium Currents

In Chaps. 6 and 8, we characterized two currents, an inward one carried by sodium ions and an outward one mediated by a potassium current. The missing member in the triumvirate of ions crucial for understanding the dynamics of the membrane potential is calcium. Ionized calcium is the most common signal transduction element in all of biology. Ca^{2+} is required for the survival of cells; yet an excess of calcium ions can lead to cell death (Johnson, Koike, and Franklin, 1992). Ca^{2+} plays a crucial role in triggering synaptic release upon the invasion of an action potential at a presynaptic site, it is the key determinant for axonal growth and muscle contraction, and it constitutes the crucial signal that initiates synaptic plasticity. Indeed, Ca^{2+} can be thought of as coupling the membrane potential to cellular output such as secretion, contraction, growth, and plasticity; that is, linking computation—as expressed by means of rapid and highly localized changes in $V_m(t)$—to action. Whenever a neuron decides to do something, Ca^{2+} is the key.

Scores of mechanisms exist to precisely adjust the concentration of free intracellular calcium $[Ca^{2+}]_i$. As we will discuss in more detail in Chap. 11, the influx of Ca^{2+} into the intracellular cytoplasm is primarily regulated by voltage-dependent calcium channels and by the NMDA synaptic receptor complex (see Sec. 4.6) in the membrane as well as by release from intracellular storage sites in the endoplasmic reticulum. These organelles are spread like a vast three-dimensional spider web throughout neurons and are thought to warehouse Ca^{2+} ions. Because the release from these intracellular storage sites usually occurs on a slow time scale, we will not discuss it here, referring the reader to Clapham (1995) for further references.

What are some of the important functional properties shared by all calcium conductances? Most importantly, the associated calcium current is always activated by depolarization, is always inward, and has some degree of inactivation that occurs on a much slower time scale than does inactivation of the sodium current. What is strikingly different among the different calcium currents is their sensitivity to depolarization. Some currents activate in response to a depolarization of a few millivolts, while others require 20 mV or even more. Some show rapid and some very slow voltage-dependent inactivation. At least three distinct flavors of voltage-dependent calcium currents have been reasonably well characterized, although as the molecular structure of calcium channels becomes better understood, we will probably be able to distinguish many more subtypes (Yang et al., 1993; McCleskey, 1994; Catterall, 1995, 1996). Finally, calcium currents are no aberrations found only in a few exceptional neurons. All nerve cells show evidence of calcium currents, many simultaneously expressing two or more types (Tsien et al., 1988). While calcium currents

appear to be largely absent in axons, they can be found throughout the dendritic tree, the cell body, and at presynaptic sites.

9.1.1 Goldman–Hodgkin–Katz Current Equation

Up to now, we have used Ohm's law to describe the relationship between sustained current flow and applied membrane potential. However, given the extreme imbalance between the typical extracellular calcium concentration, in the low millimolar range, and the intracellular concentration, ranging between 10 and 100 nM, it can be difficult to measure a reversal potential. Indeed, one would hardly expect calcium channels to generate much *outward* current beyond the calcium equilibrium potential. Even though the effective driving potential might be very large at very depolarizing values, only a few calcium ions are avilable to move into the extracellular space, making the outward current very close to zero.

The standard theoretical account for the current flowing under these conditions, based on the electrodiffusion model, was introduced into the literature by Goldman (1943) and Hodgkin and Katz (1949) (see also Secs. 4.5 and 11.3). It makes no assumption about pores, rather hypothesizing that ions move independently through the membrane along a constant electrical field (that is, a linear drop in membrane potential). Using this phenomenological model, the ionic current flowing across the membrane can be derived (see Jack, Noble, and Tsien, 1975 or Hille, 1992) to be

$$I_{Ca} = P_{Ca} 2v F \frac{[Ca^{2+}]_i - [Ca^{2+}]_o e^{-v}}{1 - e^{-v}} \tag{9.1}$$

where $v = 2V_m F/RT$ is the normalized membrane potential, with $F = 96,480$ C/mol being Faraday's constant, R the gas constant, and T the absolute temperature. P_{Ca} is the *permeability* of the membrane to calcium and is defined as the constant of proportionality between the molar flux density of calcium across a unit area of membrane S and the concentration difference across the membrane

$$S = -P_{Ca} \Delta [Ca^{2+}] \tag{9.2}$$

where the membrane permeability has units of cm/sec. (This is essentially Fick's first law of diffusion; see Eq. 11.14.) Equation 9.1 is known as the *Goldman-Hodgkin-Katz* (GHK) current equation.

If the ionic milieu on both sides of the membrane is the same, the GHK current equation is linear in the membrane potential, with a reversal potential of zero. As the external concentration increases relative to the intracellular one, the I–V curve becomes shallower and shallower for positive potentials, since it becomes increasingly more difficult for the Ca^{2+} ions to move against their concentration gradient.

For large, positive values of v, the current is linear in v, as for very negative values (e.g., $V_m < -15$ mV in the case of Fig. 9.1). The ratio of the slopes in the two domains is simply the ratio of the concentration values across the membrane.

Matching Eq. 9.1 against a real calcium current requires further considerations since, for instance, calcium channels are mildly permeable to potassium. (The ratio of the two permeabilities is 1/1000; see Lee and Tsien, 1982, and Fig. 9.1.)

Whether or not the calcium current should be described by Ohm's law or by the GHK current equation has yet to be carefully evaluated from an experimental point of view. The various numerical models that match simulations against experimental records

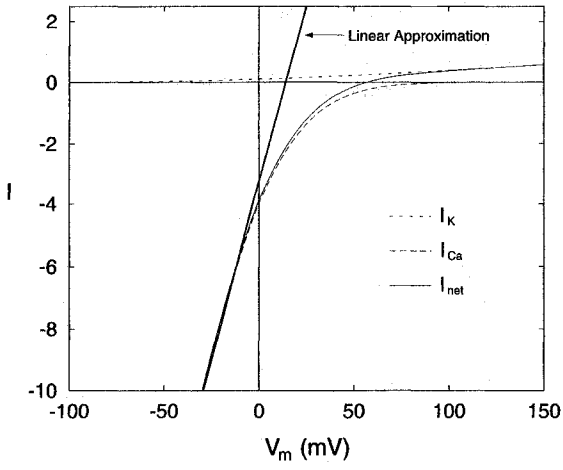

Fig. 9.1 THEORETICAL $I-V$ RELATIONSHIP FOR A CALCIUM CURRENT Due to the 40,000-fold concentration difference between extracellular Ca^{2+} (around 2 mM) and intracellular Ca^{2+} (around 50 nM), the phenomenological constant field equation of Goldman, Hodgkin, and Katz (Eq. 9.1) predicts a strongly rectifying $I-V$ relationship for calcium. If one takes account of the fact that calcium channels are also weakly selective for potassium ions, the reversal potential shifts to somewhat lower values and the curve becomes less steep, although still rectifying. A linear relationship, based upon approximating the slope of the $I-V$ curve for values $V_m < -20$ mV is superimposed. Under physiological conditions, the membrane potential almost always resides in this range. Reprinted in modified form by permission from Hille (1992).

have used either GHK or variants thereof (Llinás, Steinberg and Walton, 1981a,b; Lytton and Sejnowski, 1991; Huguenard and McCormick, 1992; DeSchutter and Bower, 1994a; Borg-Graham, 1997) or Ohm's law (Hudspeth and Lewis, 1988b; Traub and Miles, 1991; McCormick, Huguenard, and Strowbridge, 1992; Yamada, Koch, and Adams, 1998). In defense of the linear model it should be noted that under physiological conditions the cell spends almost all of its time at membrane potentials < -15 mV, a region in which the $I-V$ relationship can be approximated very well by a linear one (Fig. 9.1). Cells only briefly transgress to more positive potentials.

With this background, let us now review three of the most important calcium currents. These are not the only types of calcium currents that have been dissected out of the physiological responses of neurons. (Other currents include the P and the R calcium currents; Mintz, Adams, and Bean, 1992; Randall and Tsien, 1995.). Indeed, it remains unclear how many distinct types of ionic channels permeable to calcium ions exist in the nervous systems. This number could, potentially, be much larger than we assume today.

9.1.2 High-Threshold Calcium Current

This current, labeled L for long lasting, was for many years the only known calcium current. Different from the fast sodium current of the squid axon, $I_{Ca(L)}$ is only activated at the very depolarized levels expected during action potentials. Its halfway activation point lies around 10–0 mV (Fig. 9.2), implying that around V_{rest}, $I_{Ca(L)}$ is totally deactivated. The L current does show inactivation that is not, however, dependent on the membrane potential but depends, instead, on the intracellular calcium concentration just below the membrane. It is halfway inactivated at quite low values of $[Ca^{2+}]_i$ (tens of micromolars). Because activation

of $I_{Ca(L)}$ does not follow the onset of depolarization instantaneously but appears with a delay, the activation particle m is usually taken to the second, third, or even higher power (Hagiwara and Byerly, 1981; Johnston and Wu, 1995). Recalling the GHK equation 9.1, we can express the current as

$$I_{Ca(L)} = m(V_m)^k h([Ca^{2+}]_i) I_{Ca} \tag{9.3}$$

with k an integer ≥ 2, and I_{Ca} the GHK expression for the current as a function of the voltage (see also Kay and Wong, 1987; Hille, 1992).

Because of the existence of specific pharmacological L channel blockers, it is known that such L channels live in proximal dendrites and at the cell body of cortical pyramidal and thalamic cells (Galvan et al., 1986; Llinás, 1988; Fisher, Gray and Johnston, 1990; Westenbroek, Ahlijanian and Catterall, 1990).

9.1.3 Low-Threshold Transient Calcium Current

The low-threshold transient or T calcium current is activated at lower voltages than the L current. Typically, its half-activation point is at −40 mV. At normal resting levels, this current is turned off. It does inactivate slowly but strongly as a function of voltage, as evident in Fig. 9.3A. Under physiological conditions, the T current can be triggered by hyperpolarizing the membrane potential—thereby completely removing inactivation—and subsequently allowing synaptic input (or a depolarizing current injection) to activate it. $I_{Ca(T)}$ can generate an all-or-nothing electrical event (usually called an *LT spike*; see below) similar to a classical action potential, but much broader, on top of which two or more sodium spikes are riding (e.g., Fig. 6.1H).

In thalamic relay cells, this current has been modeled (McCormick, Huguenard, and Strowbridge, 1992; McCormick and Huguenard, 1992; Huguenard and McCormick, 1992) as

$$I_{Ca(T)} = m(V_m)^2 h(V_m) I_{Ca}\,. \tag{9.4}$$

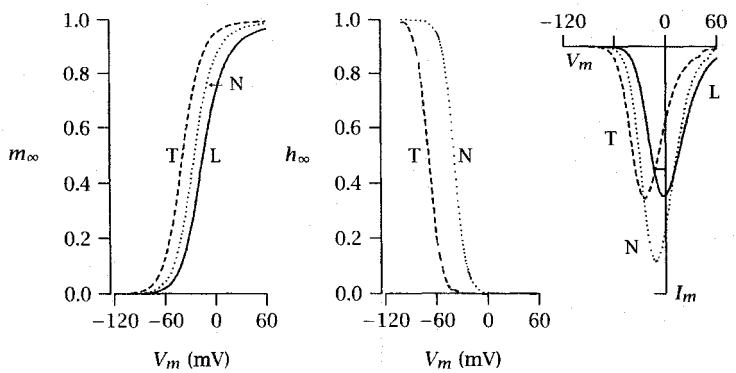

Fig. 9.2 Activation and Inactivation Ranges for Calcium Currents Steady-state activation (leftmost plot) and inactivation (middle plot) variables as a function of the membrane potential for the three calcium currents discussed in the text. Inactivation of the L calcium current does not depend on voltage but on the intracellular calcium concentration. The rightmost plot shows their I–V relationships. It is likely that intermediate forms of calcium current exist without specific pharmacological blockers to uniquely identify them. Reprinted by permission from Johnston and Wu (1995).

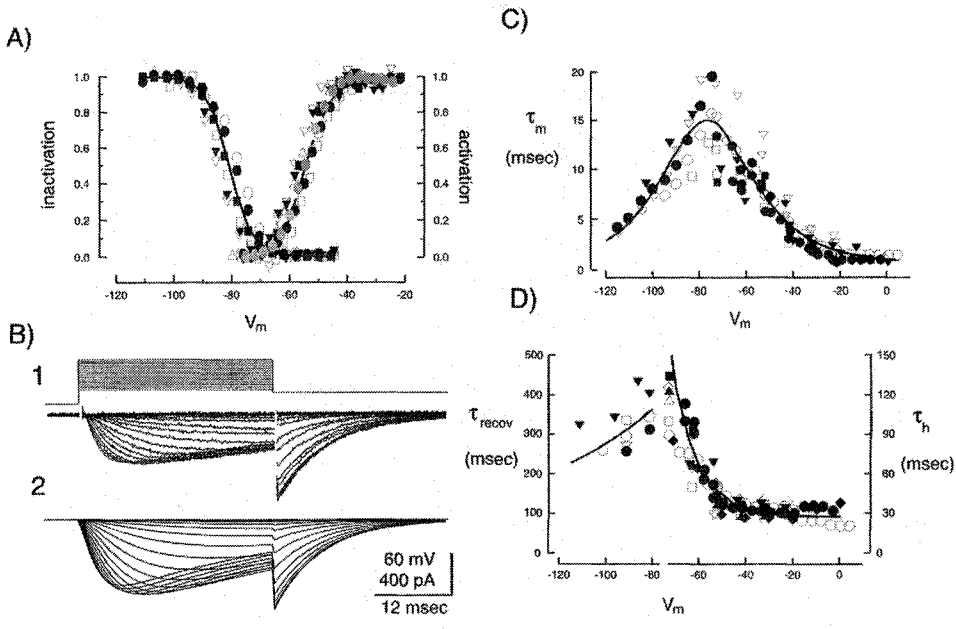

Fig. 9.3 Activation and Inactivation of the Transient Calcium Current Properties of the transient low-threshold calcium current found in rat thalamic relay cells as modeled by Huguenard and McCormick (1992) using a standard Hodgkin–Huxley-like formalism (Eq. 9.4). Data for six thalamic cells are shown. **(A)** Steady-state activation and inactivation as a function of V_m. **(B)** I_T is activated by stepping the potential for 30 msec to various potentials, followed by repolarization to −80 mV (1—experimental data; 2—model). **(C)** Time constant of activation and **(D)** of inactivation and recovery. Reprinted by permission from Huguenard and McCormick (1992).

The steady-state activation m_∞ and inactivation h_∞ as well as their associated time constants τ_m and τ_h are illustrated in Fig. 9.3 as a function of the membrane potential for the thalamus current. (For an alternate formulation see Wang, Rinzel, and Rogawski, 1991.) Different from I_{Na} in the squid axon, $I_{Ca(T)}$ does not possess a *window current.* The window current refers to current flowing at steady-state, determined by the amount of overlap between activation and inactivation at any particular membrane potential. For the T current, the window current $\overline{P}_{Ca(T)} m_\infty^2 h_\infty I_{Ca}$, is always zero or close to zero for any sustained voltages; hence its name (Fig. 9.3A). Physiological data point toward the T current as playing a prominent role in distal dendrites (Christie et al., 1995).

A significant difference between low- and high-threshold calcium currents is that the latter require depolarization beyond 0 mV, something only expected during action potentials, while the former are activated at much more modest levels of depolarization.

9.1.4 Low-Threshold Spike in Thalamic Neurons

The role that the T current might play in information transmission was first elucidated in two classical papers by Jahnsen and Llinás (1984a,b). Thalamic relay cells occupy a unique position in the central nervous system. With the exception of olfaction, all sensory systems access cortex by projecting through the thalamus (for a review see Sherman and Koch, 1986, 1998). Furthermore, about one-half of all synaptic contacts onto thalamic cells originate in the lower layers of the cortex. The thalamus is also the recipient of diffusely projecting

input from the brainstem. The various systems have more than ample opportunity to control what is transmitted through the thalamus (Crick, 1984a).

Intracellular recordings from thalamic cells in slice as well as in the intact animal (Jahnsen and Llinás, 1984a,b; Coulter, Huguenard, and Prince, 1989; Hernández-Cruz and Pape, 1989; Guido et al., 1995; Guido and Weyand, 1995) have revealed two functional, quite distinct modes of operation which are characterized by whether or not the transient calcium current is activated (Fig. 9.4).

If the membrane potential at the soma is around −75 mV or below—held there by modulatory input from the brain stem that is known to hyperpolarize thalamic cells tonically—the inactivation of $I_{Ca(T)}$ is removed and any sufficiently large depolarizing synaptic input will activate the low-threshold calcium current (Fig. 9.4A). Similar to the fast Hodgkin–Huxley-like action potential, this further depolarizes the membrane, activating additional $I_{Ca(T)}$, and so on. The result is an all-or-none action potential, the LT spike, which is relatively broad, around 50 msec. This is due to a two order of magnitude difference between fast activation and slow inactivation (Fig. 9.3D). As can be seen in Fig. 9.4A, this broad depolarization triggers a series of very fast conventional sodium spikes riding on top of the LT spike. The cell is said to *burst*; consequently, this manner of operating is known as the *burst mode*. Subsequent to the LT spike, the membrane is profoundly refractory for a period of 100 msec or longer before it can generate the next calcium spike. During the intervening period, any synaptic input will have little effect on the cell. If, conversely, the membrane is at rest or slightly depolarized, $I_{Ca(T)}$ is inactivated and any input will cause either only a subthreshold depolarization (Fig. 9.4B) or a series of conventional action potentials (Fig. 9.4C). Stronger depolarization is encoded in a higher firing frequency: the cell operates in its *relay mode*.

Steriade and his colleagues (Steriade and McCarley, 1990; Steriade, McCormick, and Sejnowski, 1993) have provided much evidence that the relatively minor dc shifts in V_m

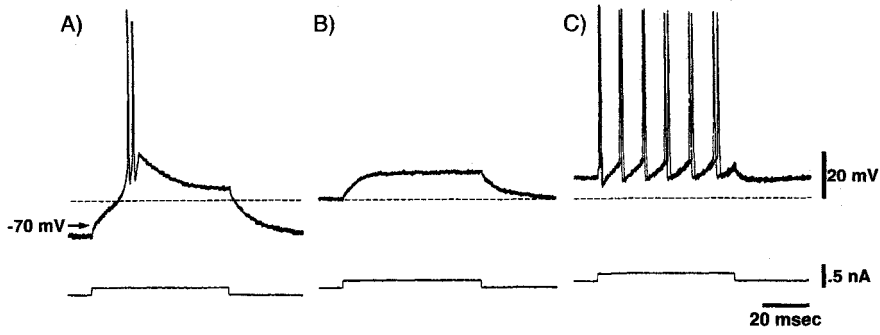

Fig. 9.4 BURSTING IN THALAMIC NEURONS The majority of thalamic cells can be in one of two functionally quite distinct states. **(A)** If the membrane potential is tonically hyperpolarized to −75 mV or beyond—due to modulatory activity from the brainstem or inhibitory synaptic input—a transient low-threshold calcium current is de-inactivated. A depolarizing current step (indicated in the lower trace) triggers a slow all-or-none electrical event due to inward calcium current, the so-called LT spike. Riding on top of the LT action potential are a number of conventional, fast sodium spikes. The LT spike concludes with a profound hyperpolarization that prevents excitatory synaptic input during this time from generating output spikes. **(B)** In an intermediate state, the cell responds to the same input in a linear fashion, with a slowly rising and decaying depolarization. **(C)** If the membrane is tonically depolarized to −60 mV or above, the same input causes the cell to fire a series of conventional fast sodium action potentials. This constitutes the so-called *relay mode*. Reprinted in modified form by permission from Jahnsen and Llinás (1984a).

which bring about the switch from one mode into the other are controlled by modulatory input from a small number of discrete sites in the brainstem. It is known that thalamic cells in anesthetized as well as in awake behaving cats can respond to visual stimuli using burst as well as isolated spikes, preferentially generating bursts during the early phase of fixation (Guido and Weyand, 1995; Guido et al., 1995). We will return in Sec. 16.3 to the possible significance of bursting for information processing.

9.1.5 N-Type Calcium Current

This is a current that has properties intermediate between the L and the T calcium currents, hence its name N for neither L nor T. It is activated at potentials intermediate between the low- and high-threshold currents (Fig. 9.2). It does show slower, voltage-dependent inactivation dynamics than the T current and has a specific pharmacological channel blocker. The N current is modeled as

$$I_{\mathrm{Ca(N)}} = m(V_m)^3 h(V_m) I_{\mathrm{Ca}} \tag{9.5}$$

(see Sutor and Zieglgänsberger, 1987; Lytton and Sejnowski, 1991).

Westenbroek and colleagues (1992) stained the entire rat brain with antibodies to a part of the N channel. As expected, most gray matter through the central nervous system was stained, in particular proximal and distal dendrites and presynaptic terminals. Thus, N channels appear to complement the locations of L channels, which are restricted to the cell bodies and the proximal dendrites of pyramidal cells (Westenbroek, Ahlijanian, and Catterall, 1990).

9.1.6 Calcium as a Measure of the Spiking Activity of the Neuron

No matter through which type of calcium channel Ca^{2+} ions enter the neuron, they will now diffuse throughout the available space and interact with enzymes and proteins in the membrane and the cytoplasm. We defer until Chap. 11 an in-depth account of the mathematics of diffusion and binding. Nonetheless, let us here briefly allude to a computationally interesting role of intracellular calcium.

Around the intracellular mouth of calcium channels, Ca^{2+} exit the 5 Å pore at rates exceeding one million per second. These ions diffuse throughout the neuron, binding at available sites in the cytoplasm and the intracellular organelles (this binding can induce release of Ca^{2+} ions from these organelles). While the majority of Ca^{2+} ions is bound, a small amount remains unbound and slowly accumulates inside the cytoplasm. Each action potential admits further calcium ions which further increases $[Ca^{2+}]_i$. This buildup is illustrated in numerical simulations of the spherical cell body of bullfrog sympathetic ganglion cells (Fig. 9.5; see Gamble and Koch, 1987, and Sec. 9.4 below). The Ca^{2+} ions rushing in through calcium channels for the few milliseconds that these channels are open during an action potential, increase $[Ca^{2+}]_i$ in the core of the cell by between 3 and 4 nM. To a first order, this increase is relatively independent of the spiking frequency (here varying between 10 and 50 Hz). While 3 nM might appear as a tiny increase, it is averaged over the entire cell body and will be much larger in local regions. The increase needs to be judged against the low resting level of $[Ca^{2+}]_i$, between 10 and 50 nM.

Experimental calcium measurements in cell bodies of the sea snail *Aplysia* (Gorman and Thomas, 1980), of bullfrog sympathetic ganglion cells (Smith, MacDermott, and Weight, 1983; Hernández-Cruz, Sala, and Adams, 1990) and of cortical pyramidal cells (Fig. 9.6; Helmchen, Imoto, and Sakmann, 1996) have confirmed this hypothetical buildup, which

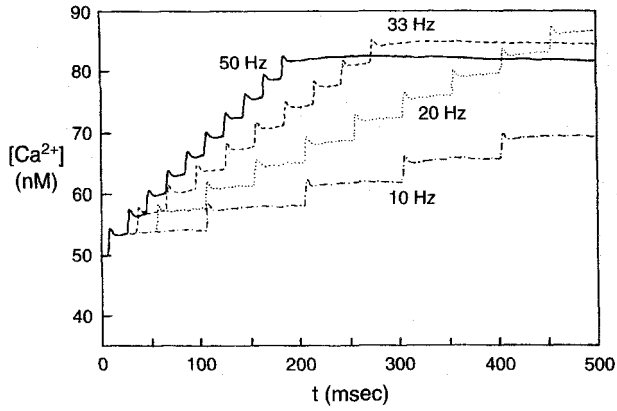

Fig. 9.5 INTRACELLULAR CALCIUM ACCUMULATION FOLLOWING SPIKING ACTIVITY Increase in intracellular free calcium in simulated bullfrog sympathetic ganglion cells in response to repetitive fast synaptic input at different input frequencies. For a more detailed description of this model see Sec. 9.4. The increase of $[Ca^{2+}]_i$ in the central 19-μm-radius core of the 20-μm-radius cell body is relatively independent of the spiking frequency (each synaptic input triggers one spike). In other words, the calcium concentration provides an index for the spiking activity of the cell in recent times. (The time constant of this integrated measure depends on the cellular geometry; the larger the volume, the longer the effective time constant; see Sec. 11.7.2.) This "activity" measure can be read out by any calcium-dependent enzyme or protein. Reprinted by permission from Gamble and Koch (1987).

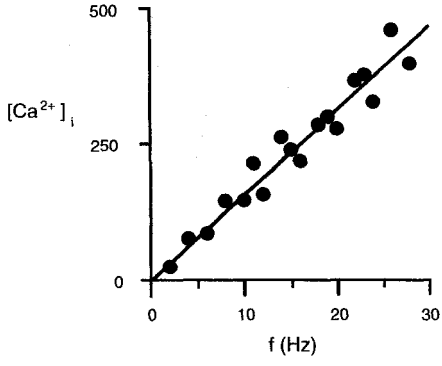

Fig. 9.6 CALCIUM BUILDUP PROPORTIONAL TO NEURONAL ACTIVITY Following each action potential in a layer 5 pyramidal neuron, calcium rushes into the cell and accumulates, here recorded using a calcium-dependent fluorescent dye in the proximal apical dendrite (Helmchen, Imoto, and Sakmann, 1996). This increase in calcium reaches an equilibrium with a time constant of 200 msec. The final level (in nM) is linearly related to the firing frequency of the cell (evoked by current injections), with a slope of 15 n*M*/Hz (solid line). Reprinted in modified form by permission from Helmchen, Imoto, and Sakmann (1996).

reaches a plateau between 0.1 and 1 sec, depending on the geometry of the cell. It gradually subsides due to extrusion processes that remove the excess calcium from the cytoplasm.

The integrated measure of past neuronal activity can be *read out* by any enzyme or protein that is sensitive to calcium, such as a calcium-dependent potassium channel (see below), or any of the myriad cellular processes that are so exquisitely sensitive to calcium concentration (see Chaps. 11 and 20). This allows the neuron or a local circuit to up or downregulate its own activity (a sort of *gain control* operation). Indeed, experimental evidence has accumulated in favor of this *calcium set-point* hypothesis, in which the concentration of free, intracellular calcium determines the amplitude of various ionic currents (Johnson, Koike, and Franklin, 1992; Turrigiano, Abbott, and Marder, 1994). An elegant modeling study has shown us how

a simple neuronal system, here modeled by the Morris-Lecar equations (Sec. 7.2), can be modified to adjust its maximal conductances $\overline{G}$ as a function of integrated calcium activity until the system expresses stable spiking patterns (LeMasson, Marder, and Abbott, 1993).

9.2 Potassium Currents

A variety at least as great as among the calcium channels, if not greater, is displayed by ionic channels permeable to potassium ions. Under physiological conditions, current flow through these channels is outward, that is, upward in the normal convention. Given the physiological reversal potential of K^+ in the neighborhood of -100 mV, potassium currents can be thought of as stabilizing the membrane potential, since activating a potassium current pulls the membrane potential to hyperpolarizing levels. As we saw already in the case of I_{DR}, the delayed rectified potassium current in the squid axon (Sec. 6.2.1), potassium currents serve to keep the action potential brief. In the absence of such a potassium current, which rapidly repolarizes the membrane, the action potential would be much longer and would follow the time course of inactivation of the sodium channel.[1] As we will see, potassium currents serve to delay the generation of an action potential following synaptic or current input as well as to reduce the firing frequency in the face of a constant input.

Like the majority of ionic currents, potassium currents—with the noticeable exception of the anomalous or inward rectifier current (Hagiwara, 1983; Doupnik, Davidson, and Lester, 1995)—require depolarization to activate. Around V_{rest}, they—as well as all sodium and calcium currents—are very small, minimizing the possibly wasteful antagonistic inward and outward current flow and, thereby, metabolic cost. In a sense, biology might have discovered a principle that designers of portable computers only implemented within the last few years: when not in use, reduce the clock rate of the microprocessors as much as possible in order to conserve precious battery power.

9.2.1 Transient Potassium Currents and Delays

Next to I_{DR}, arguably the most important potassium current is a transient, inactivating potassium current, known as I_A. First characterized by Connor and Stevens (1971b), it lives in a rather narrow voltage range between -70 and -40 mV, activating within 5–10 msec. Different from the delayed rectifier, I_A inactivates on a slower time scale, typically on the order of 100 msec. Based on their voltage-clamp data, Connor and Stevens (1971c) described I_A on the basis of Ohm's law,

$$I_A = \overline{G}_{K(A)} m(V_m)^4 h(V_m)(V_m - E_K) . \tag{9.6}$$

The fourth power yields the observed sigmoidal activation curves, while the single inactivation particle reflects the exponential decay of the current. The time constants of activation and inactivation depend only weakly on the membrane potential.

The functional relevance of I_A (Connor and Stevens, 1971c) can be understood by reference to Fig. 9.7. As we learned in Chaps. 6 and 7, the squid axonal membrane shows an abrupt onset of spiking: in the standard model, the minimum spiking frequency is 53 Hz. We can understand why either by looking at the exact equations or by considering phase space analysis. In terms of biophysics, the Hodgkin–Huxley equations are unable to

1. An exception to this are the nodes of Ranvier of myelinated fibers, in which a vigorous leak current serves to partially repolarize the membrane; Sec. 6.6.

generate spikes at very low frequencies, since too slow a rate of depolarization would lead to inactivation of the sodium current. In Chap. 7 we used phase space analysis to argue that onset of oscillations with an infinitely long period requires a saddle-node bifurcation that can be obtained with the help of an inactivation variable that depends steeply on the membrane potential (witness the $\dot{w} = 0$ nullcline in Fig. 7.9).

I_A exactly fulfills this condition: it is active in a narrow subthreshold range. In cortical pyramidal cells—such as the one modeled in Fig 9.7—this current will try to hyperpolarize the membrane potential subsequent to a current step (hence the bump in Fig. 9.7A; Segal and Barker, 1984; Schwindt et al., 1988; Zona et al., 1988). In this voltage range, I_A slowly inactivates, thereby contributing less and less outward current: V_m slowly drifts upward until the spiking threshold is reached and a spike is triggered. A similar mechanism generates delays of up to 3–4 sec in molluscan neurons (Getting, 1983). It has also been hypothetized that a class of cells in the cat lateral geniculate nucleus, *lagged cells*, which show a much delayed response to a visual stimulus compared to nonlagged geniculate cells, implement this delay via a transient A current (Saul and Humphrey, 1990; McCormick, 1991).

I_A can exert another profound effect on the firing behavior of cells. As is apparent upon inspection of the f–I curve of a patch of squid axon membrane (Fig. 6.10A), the bandwidth

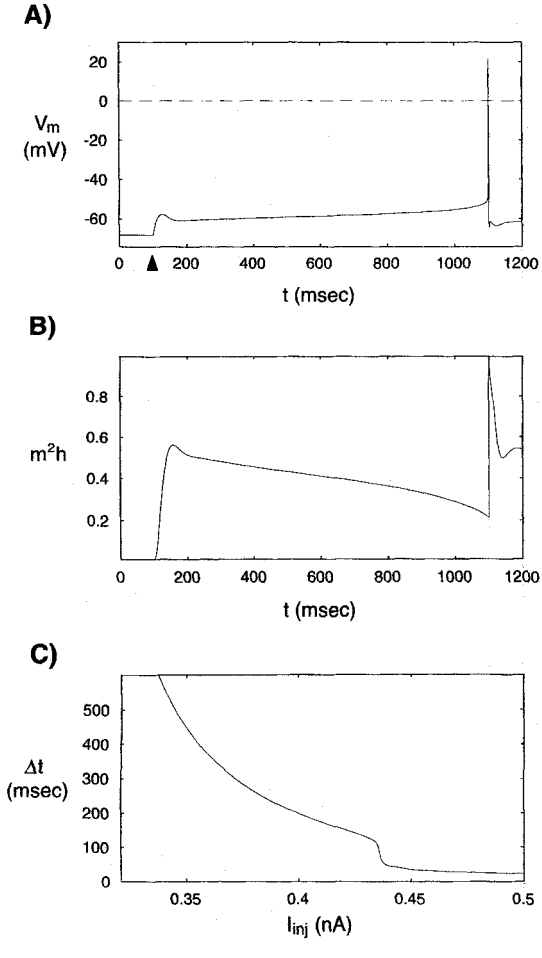

Fig. 9.7 DELAYED SPIKING DUE TO TRANSIENT POTASSIUM CURRENT The A current implements a delay element. **(A)** Somatic membrane potential in the standard pyramidal cell model in response to a 0.32-nA current step injected at 100 msec. V_m depolarizes and activates the transient potassium I_A current. At these potentials I_A slowly inactivates, as evident in **(B)**, showing the normalized A conductance. (An m^2h instead of the m^4h formalism of Eq. 9.6 was used.) This gradual inactivation of a potassium current allows the membrane potential to creep upward until, 1 sec after the current injection, an action potential is generated. Without I_A the membrane potential would either remain subthreshold or generate a spike within a few tens of milliseconds. **(C)** Relationship between the injected current and the delay between current onset and spike initiation.

of firing is very limited because of the high onset firing frequency. The remedy for this is the introduction of I_A, allowing the membrane to generate action potentials across a much larger firing frequency range than before.

The A current is just one member of a larger class of transient inactivating potassium currents that share similar pharmacological and functional properties (Rudy, 1988). Other members of this club include I_D (D for delay) described in hippocampal cells (Storm, 1988) and I_{As}, found in thalamic neurons (McCormick, 1991). Both currents have very long activation times, causing a delay in the onset of spiking in response to a current injection of up to 10 sec.

We conclude that I_A and its siblings subserve at least two functions: (1) to allow cells to fire at very low frequencies, thereby increasing the bandwidth of the firing frequency code significantly, and (2) to implement a delay element that does not require ultraslow intrinsic time constants.

9.2.2 Calcium-Dependent Potassium Currents

The amplitude of several potassium currents is influenced by $[Ca^{2+}]_i$, the intracellular concentration of Ca^{2+} ions. These currents are collectively referred to as $I_{K(Ca)}$ to emphasize that they are modulated by calcium but that the current itself is carried by K^+ ions. The function of these currents is to shape the membrane potential following individual action potentials (Fig. 9.8), to read out the previous spiking history of the cell, shaping adaptation accordingly, and to instantiate, in conjunction with a calcium current, a resonance-like behavior (Hudspeth and Lewis, 1988b; Sec. 10.4.3).

We here discuss two potassium currents: I_C and I_{AHP} (Latorre et al., 1989).

I_C is a fairly large, outward current whose activity depends on $[Ca^{2+}]_i$ as well as on V_m. I_C quickly activates upon the entry of calcium through calcium channels during an action potential. Similar to the delayed rectifier, it rapidly repolarizes the membrane potential, shutting off in the process in readiness for the next spike. It is not easy to study the dynamics

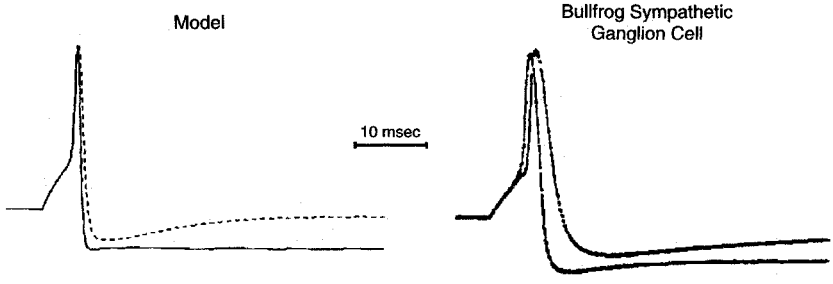

Fig. 9.8 Calcium and the Action Potential Effect of blocking calcium channels on computer-simulated and observed action potentials in type B bullfrog sympathetic ganglion cells (Yamada, Koch, and Adams, 1998). In both cases, the standard action potential (induced by a brief current pulse) repolarizes more quickly and is followed by a longer afterhyperpolarization than the action potential (dotted lines) in the absence of calcium currents (achieved in the experiment by adding cadmium to the bathing solution and in the model by reducing $\overline{G}_{Ca}$ to 5% of its normal value). The effect of blocking Ca^{2+} on the peak amplitude of the spike is minimal: the spike itself is mediated by Na^+ and not by Ca^{2+} ions. Reprinted in modified form by permission from Yamada, Koch, and Adams (1998).

of this, or any other calcium-dependent potassium current, since its time course is highly sensitive to the calcium concentration in the immediate neighborhood of the underlying channel. Because Ca^{2+} will decay very differently in thin dendrites than in a large cell body, I_C will also have a different time course, even if the dynamics of the membrane potential are the same in both cases.

The microscopic gating of the ionic channels underlying this current has been studied in some detail, giving rise to complex kinetic gating schemes with two or more calcium ions necessary for the channel to open (McManus and Magleby, 1988). A much simpler gating scheme for the underlying conductance g_C that reproduces much of the time and voltage dependency involves calcium ions binding to a single activation particle, which effects the transition from closed to open channel in a voltage-dependent manner (Adams et al., 1986; Yamada, Koch, and Adams, 1998):

$$I_C = \overline{G}_C m(V_m, [Ca^{2+}]_i)(V_m - E_K) . \tag{9.7}$$

If I_{DR} and I_C were the only currents activated by a single action potential, the spike afterhyperpolarization (AHP) would promptly return to rest with a time course dictated by the membrane time constant. Yet neurons throughout the nervous system (Connors, Gutnick, and Prince, 1982; Pennefather et al., 1985; Lancaster and Adams, 1986) show a second component of the AHP, reflecting a much smaller and slower calcium-dependent potassium conductance. The associated current, termed I_{AHP}, is small and depends only on the concentration of intracellular calcium just below the membrane. The secret to its success is that it is sustained: when calcium rushes in during an action potential, I_{AHP} turns on and effectively subtracts from the depolarizing current from an electrode or from synaptic input. In hippocampal pyramidal cells, the amplitude of the hyperpolarization following spiking activity increases with increasing number of action potentials, showing that I_{AHP} increments with each spike (Madison and Nicoll, 1984). Blocking this current prevents firing frequency adaptation from occurring. The current is described as

$$I_{AHP} = \overline{G}_{AHP} m([Ca^{2+}]_i)(V_m - E_K) . \tag{9.8}$$

Experimentally, I_{AHP} can be distinguished from I_C by the use of naturally occurring toxins that are added to the solution bathing the neurons: while I_C is blocked in many cells by charybdotoxin, a peptide from scorpion venom, I_{AHP} can be blocked by injecting a toxin from bee venom, apamin. This reveals the tight coevolution of predators and the nervous systems of the animals they hunt.

9.3 Firing Frequency Adaptation

Throughout neocortex, hippocampus, and thalamus, cells receive a clearly defined input from a single site in the pontine brainstem, the *locus coeruleus*. Each of the small number of coeruleus neurons (about 2 × 1600 in rat and 2 × 13,000 in humans) projects in a very diffuse manner throughout the brain. A single neuron might enervate frontal cortex, thalamus as well as occipital cortex (Foote and Morrison, 1987). Excitation in these cells has been related to increased vigilance and arousal in both rats and monkeys (Foote, Aston-Jones and Bloom, 1980).

Upon stimulation, the terminals of these neurons release the neurotransmitter *noradrenaline* (also termed norepinephrine) onto their postsynaptic targets (see Table 4.1). This leads to a quite pronounced and long-lasting change in the excitability of these cells, an effect

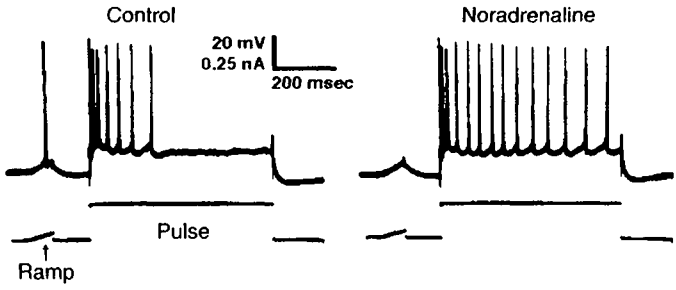

Fig. 9.9 Slow Modulation of Firing Frequency Change in firing frequency adaptation in CA1 pyramidal cells from a hippocampal slice during application of noradrenaline. A brief just-threshold current ramp is applied first, followed by a 650-msec-long, suprathreshold current pulse. The principal action of noradrenaline, mediated by a second messenger, is to reduce firing frequency adaptation by blocking the slow calcium-dependent potassium conductance I_{AHP}. A side effect is a slight increase in the firing threshold of the cell (that is, the brief current ramp does not trigger an action potential in the presence of noradrenaline). This modulation in the firing properties can persist for seconds or even minutes. Hippocampal pyramidal cells receive a well-defined noradrenergic input from brainstem neurons. Reprinted by permission from Madison and Nicoll (1986).

that has been studied in isolation in pyramidal cells in the neocortical and the hippocampal slice preparation (Madison and Nicoll, 1986; Nicoll, 1988; Schwindt et al., 1988).

Application of noradrenaline to pyramidal cells causes two changes. One is a small (about 2–3 mV) hyperpolarization, leading to a measurable *increase* in the spiking threshold (Fig. 9.9). A much more dramatic effect can be observed when the cell is sufficiently excited to fire trains of spikes. Normally, these cells adapt, that is, their firing rate in response to a constant current step slows down (as in "Control" in Fig. 9.9). In the presence of noradrenaline, spike discharge accommodation is almost completely blocked. Its action is specific in that neither the shape of the action potential itself nor the fast afterhyperpolarization phase is affected. Indeed, experiments have shown (Madison and Nicoll, 1986) that noradrenaline specifically blocks I_{AHP} for many tens of seconds. This effect is mediated by a metabotropic receptor (Sec. 4.4 and Table 4.2). In this case, noradrenaline binds to β_1 adrenergic receptors, releasing a second messenger inside the cell which directly or indirectly phosphorylates the channel proteins underlying I_{AHP}. An added complication is that the small hyperpolarizing action of noradrenaline—caused by an *increase* in a potassium conductance— is mediated by α adrenergic receptors. Any neuroactive substance in the brain will often initiate a series of changes in the electrical behavior of its postsynaptic targets via multiple actuators (here receptors).

Noradrenaline is not alone in being able to control spike rate adaptation in cortical cells. Acetylcholine, mediated by a dense cholinergic input to the hippocampus from cells in the medial septal nucleus, has a similar effect, although its action is even more complex than that of noradrenaline (it appears to modify at least four distinct potassium currents; Cole and Nicoll, 1984; McCormick and Prince, 1986; Nicoll, 1988; Schwindt et al., 1988). The pyramidal cells that receive such a cholinergic input can have their spike rate accommodation switched off for tens of seconds in the absence of any direct change of the membrane potential.

The lesson is that multiple, diffusely projecting systems in the brain can independently control the excitability of neurons via slow modulation of membrane conductances. Their mode of action is somewhat similar to a *broadcast* that is sent out to all processors in a

massively parallel computer. In other words, all processors will receive the same signal. Because a single neuron in the locus coeruleus projects widely throughout the brain, this blockage of spike rate adaptation is not very precise in terms of space nor in terms of time (since it typically requires a fraction of a second to set in and may last for many, many seconds). From a computational point of view, these diffuse systems that target specific conductances should be thought of as modifying the basic electrical properties of the processing circuits on a relatively global scale, possibly for controlling the level of arousal or vigilance and for providing a single slow global feedback signal during learning.

9.4 Other Currents

Besides the handful of voltage-dependent membrane currents discussed so far, there exist a plethora of other currents that are responsible, in isolation or in concert with others, for shaping various phases of cellular excitability (Llinás, 1988). They include I_M, a slowly changing voltage-dependent potassium current found in pyramidal cells, which contributes to the accommodation of action potential discharge (Halliwell and Adams, 1982; Brown, 1988), as well as an entire family of inward rectifier potassium currents, which are activated upon hyperpolarization of the membrane potential (Hagiwara, 1983; Spain, Schwindt, and Crill, 1987).

A smaller and less well understood family of channels is primarily permeable to chloride ions, by far the most abundant anions in biological systems (Hille, 1992). In general, the reversal potential for Cl^- is within 10–15 mV of the resting potential of neurons, and activation of a chloride current will repolarize the cell and prevent it from firing. The voltage and time dependencies of chloride conductances are only minor and slow. Therefore, they probably contribute to the leak conductance that is usually assumed to be independent of the applied membrane potential. There also exists a calcium-activated chloride conductance with only a weak voltage dependency, which could play a similar role to calcium-dependent potassium conductances (Mayer, 1985).

A possible important current is the *sustained* or *persistent sodium current* $I_{Na,p}$. It has been clearly documented in cortical pyramidal cells (Stafstrom et al., 1985; French et al., 1990) due to the sensitivity to TTX that it shares with its fast sibling, I_{Na}. This current turns on within a few milliseconds upon depolarization, but either does not inactivate at all or only very slowly, thereby providing a steady inward current. Because $I_{Na,p}$ is activated near the resting potential, it tends to amplify small EPSPs. The firing frequency of the cell will be quite sensitive to the total amount of this current, since too much $I_{Na,p}$ will prevent repolarization following action potentials.

9.5 An Integrated View

For the most part, this chapter has described individual currents and their possible functional roles. Before we go on to other matters, we would like to give the reader a holistic view of how these different currents interrelate and how they function within an entire system. As example, we will discuss the simulacrum of type B bullfrog sympathetic ganglion cells of Adams et al., (1986) and Yamada, Koch, and Adams (1998). These neurons make only a lowly contribution to the overall scheme of things, enabling the animal to control its glands for slime production. From an electrophysiological point of view, though, these cells are

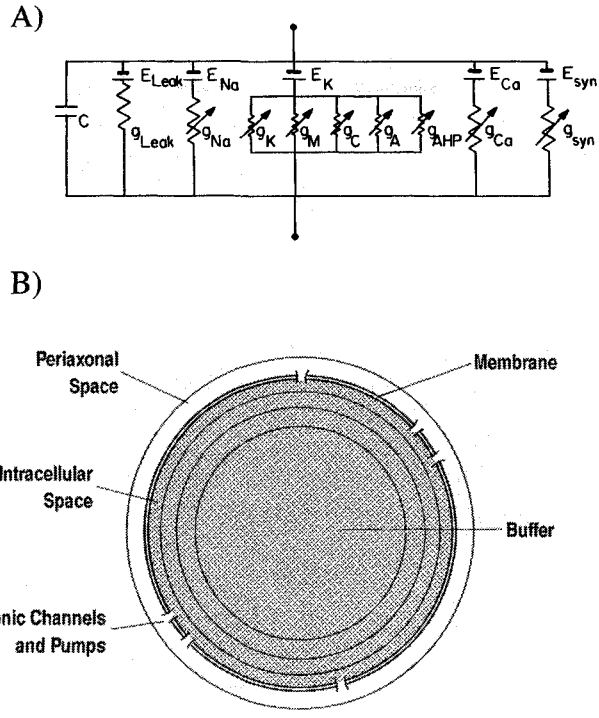

Fig. 9.10 Modeling a Bullfrog Sympathetic Ganglion Cell **(A)** Electrical circuit used in the Yamada, Koch, and Adams (1998) simulacrum of type B bullfrog sympathetic ganglion cells. Given their spherical shape and the complete absence of any dendrites, a single lumped compartment that includes seven time-, voltage-, and calcium-dependent membrane conductances is entirely sufficient to model their electrical behavior. **(B)** Underlying assumptions for modeling the extracellular accumulation of potassium (in a single extracellular compartment) and the series of shells surrounding a well-mixed central core to account for Ca^{2+} diffusion inside the cell. A calcium buffer is distributed throughout the cell. Not drawn to scale. Reprinted by permission from Yamada, Koch, and Adams (1998).

ideal since they are easy to cultivate, big (with a mean diameter of 35 μm), and devoid of any dendritic processes.

The electrical structure of the model, shown schematically in Fig. 9.10, includes the seven time-, voltage-, and calcium-dependent conductances found in these cells, in addition to a passive RC contribution: the fast sodium I_{Na} and the delayed rectifier potassium I_{DR} currents underlying spike production, an L type calcium current I_{Ca}, the two forms of calcium-dependent potassium currents discussed above, I_C and I_{AHP}, the transient potassium current I_A, and a fifth potassium current, the small and slowly activating voltage-dependent M current. The description of these currents is derived from voltage-clamp data and is based on the conventional Hodgkin–Huxley rate formalism and the use of Ohm's law. (for the numerical values of all parameters, consult the appendix in Yamada, Koch, and Adams, 1998). Because of the spherical geometry of these cells, they are electrically compact and can be modeled using a single compartment.

Sympathetic ganglion cells are *not* compact from the point of view of the spatio-temporal distribution of the Ca^{2+} ions entering the cell via calcium channels. As treated in detail in

Chap. 11, the diffusion equation is solved in spherical coordinates, using a series of thin shells surrounding a well-stirred, central core. Ca^{2+} ions can bind to a stationary buffer distributed throughout the cytoplasm using a second-order reaction (see Sec. 11.4.1). In the outermost compartment just below the membrane, calcium ions are extruded from the cell via a first-order calcium pump. Finally, in order to account for the accumulation of potassium ions in the pericellular space just outside the neuronal membrane—leading to a significant reduction of the potassium battery E_K following spike activity—the cell is assumed to be surrounded by a single compartment, whose concentration of K^+ ions is determined by a simple uptake mechanism. We leave the mathematics of solving two coupled sets of nonlinear equations for $V_m(t)$ and $[Ca^{2+}](x, t)$ to Appendix C.

Figures 9.11 and 9.12 illustrate the basic performance of the model in response to a short current pulse that triggers an action potential. The spike itself (Fig. 9.8) is similar to the squid axon spike (Fig. 6.6) with the noticable exception of the second, long-lasting phase of the afterhyperpolarization, mediated by I_{AHP}. Moreover, in these cells I_C, rather than I_{DR}, is largely responsible for repolarizing the potential following the excursion of V_m to 0 mV and beyond (as can be ascertained by comparing the peak amplitudes of I_C and I_{DR}).

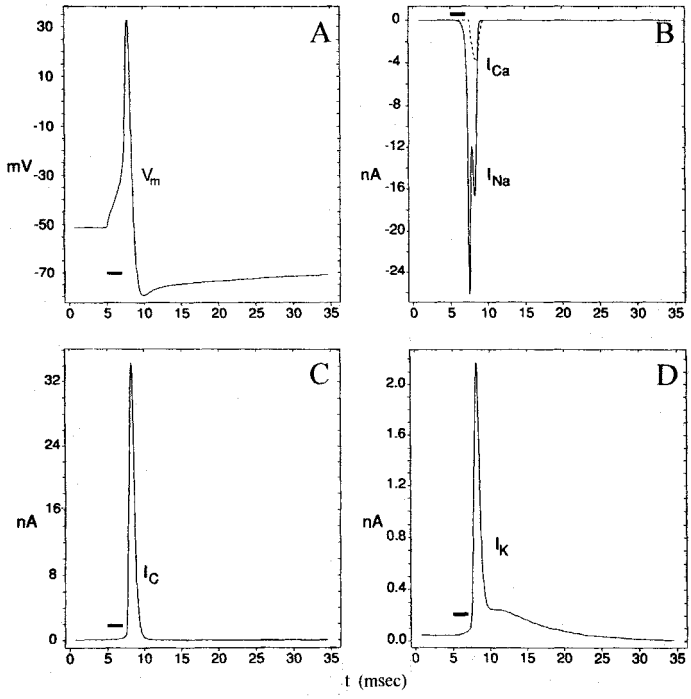

Fig. 9.11 Response of the Sympathetic Ganglion Cell Model: Major Currents Response of the bullfrog sympathetic ganglion cell model (see Fig. 9.10) at rest to a 2-msec-long current pulse of 1.75-nA amplitude (indicated by black bars). This panorama depicts the major currents involved in spike initiation and repolarization seen in **(A)** (identical to the spike in Fig. 9.8). Notice the fast and slow components of the afterhyperpolarization. The two inward currents I_{Na} and I_{Ca} are plotted in **(B)**. Only 9% of the incoming charge is carried by Ca^{2+} ions, emphasizing the fact that the primary function of calcium ions is to shape neuronal excitability, rather than to be directly involved in spike production. **(C)** Fast calcium-dependent potassium current I_C that contributes substantially more to spike repolarization than the delayed rectifier current I_{DR}, shown in **(D)**. Reprinted by permission from Yamada, Koch, and Adams (1998).

The amplitude of I_{AHP} is minute compared to I_C; yet, because it is maintained, it has a crucial role to play in determining spike accommodation (Adams et al., 1986). Changes in the driving potential can be quite significant, as seen in the transient 50 mV reduction in E_{Ca} (Fig. 9.12B) caused by the very brief elevation of $[Ca^{2+}]_i$ just below the membrane to micromolar values.

The effect of blocking either I_M or I_{AHP} or both on the average firing frequency is the subject of Fig. 9.13. Blocking I_{AHP} leaves the current threshold for spike initiation unchanged but does increase the gain of the f–I curve by about a factor of 2. Exactly the same result is observed in a quite different system, vestibular neurons in the brainstem (du Lac, 1996; Fig. 21.3) where pharmacological elimination of the slow calcium-dependent potassium current increases the gain of the f–I curve by a factor varying between 1.38 and 2.28.

Blocking but I_M in the bullfrog leaves the slope of the discharge curve relatively unchanged while reducing I_{th} to 5% of its original value. Removing both conductances

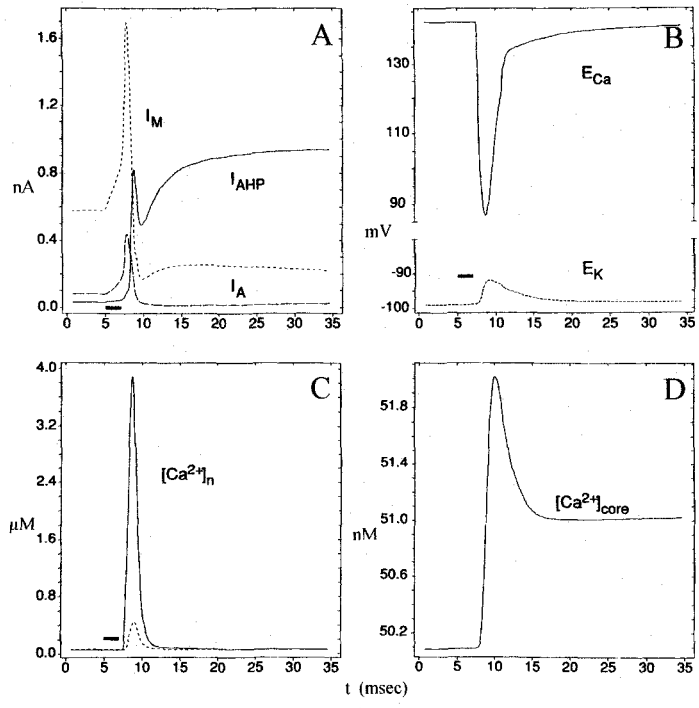

Fig. 9.12 Response of the Sympathetic Ganglion Cell Model: Minor Currents and Calcium Concentration Response of the bullfrog sympathetic ganglion cell to the same stimulus as in Fig. 9.11. **(A)** Three smaller potassium currents I_M, I_{AHP}, and I_A. The latter does not appear to play any significant role in these cells. I_M is active at rest. The primary effect of blockage of I_M is a reduction in current threshold I_{th}, while blockage of I_{AHP} leads to a partial loss of spike firing adaptation. Blockage of both currents occurs *in vivo* during stimulation of cholinergic input to the ganglia. The changes in the Nernst potentials for E_{Ca} and E_K are shown in **(B)**. The primary rapid and the secondary slow components in the change in E_{Ca} reflect the rapid increase in free calcium concentration in the outermost shell just below the membrane plotted in **(C)**. Activation of I_{Ca} leads to a rapid influx of Ca^{2+} ions that quickly bind to the buffer. The slow decay results from calcium loss via the pump as well as diffusion toward the core of the cell. $[Ca^{2+}]_i$ for the tenth shell below the membrane (dotted line) is also illustrated in **(C)**. The calcium concentration in the central core is shown in **(D)**. Reprinted by permission from Yamada, Koch, and Adams (1998).

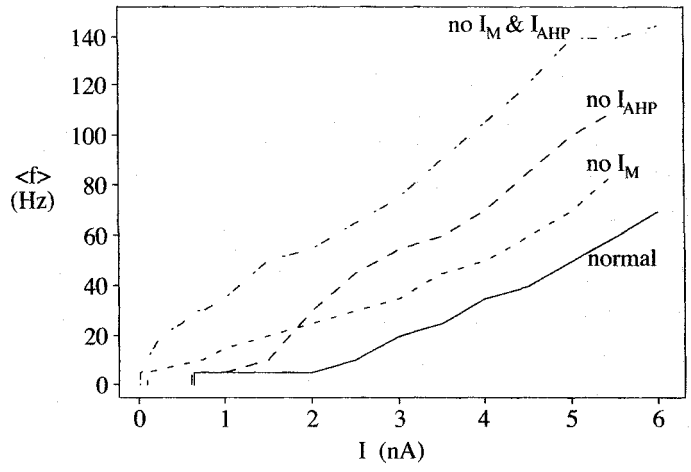

Fig. 9.13 CHANGING THE GAIN OF THE DISCHARGE CURVE Effect of blocking either I_M or I_{AHP} or both on the $f-I$ curve of the model bullfrog sympathetic ganglion cell. Mean firing rate, averaged over 200 msec, following current steps of variable amplitude. Removing I_M primarily affects I_{th} but leaves the slope intact, while eliminating I_{AHP} increases the gain of the discharge curve by a factor of 2. Blocking the two simultaneously leads to the summation of both effects. The control of the gain of a neuron via control of the amount of the slow calcium-dependent potassium current present might be a crucial biophysical operation underlying different computations. Reprinted by permission from Yamada, Koch, and Adams (1998).

lowers the current threshold but increases the slope, leading to the dramatic removal of spike adaptation observed experimentally (Adams et al., 1986).

If I_{AHP} can be controlled in individual neurons, rather than by a globally acting neurotransmitter such as noradrenaline, as introduced above, it offers the possibility of selectively up or down regulating the gain of a neuron without affecting the spike generation mechanism itself. Given the importance of receptive field models that incorporate a multiplicative effect on the gain of individual neurons (leading to so-called *gain fields*; Zipser and Andersen, 1988; but see Pouget and Sejnowski, 1997), this might be a crucial canonical biophysical operation.

9.6 Recapitulation

In this chapter, we summarized some of what is known about ionic currents populating the nervous system other than I_{Na} and I_{DR} of squid axon fame. In particular, we introduced calcium currents. Ca^{2+} ions are crucial for the life and death of neurons; they link rapid changes in the membrane potential, used for computation, with action, such as neurotransmitter release at a synapse, muscle contraction, or biochemical changes underlying cellular plasticity. Three broad classes of calcium currents are known: L, T, and N currents, although it is unclear whether these are just three samples along a continuum of such currents. Because of the substantial imbalance between the concentration of Ca^{2+} inside and outside the cell, electrical rectification needs to be taken account of. Typically, this requires the use of the Goldman-Hodgkin-Katz equation to describe calcium currents, rather than the linear Ohm's law. The accumulation of calcium ions following action potential activity has the useful function that the intracellular calcium concentration in the cell represents an index of the

recent spiking history of the cell. Various proteins and enzymes, such as calcium-dependent potassium channels, might be able to read out this variable and use it to normalize excitability or for gain control.

While calcium ions themselves play almost no role in generating conventional action potentials, calcium currents can support a slower all-or-none electrical event, the LT spike, leading to a burst of fast sodium spikes. It may be possible that these and other forms of bursts represent events of special significance in the nervous system.

We introduced some of the many potassium currents that have been identified, focusing on the transient inactivating potassium current I_A. It serves to linearize the discharge curve around threshold and implements a delay element between the onset of depolarizing input and spike initiation. It does so via a voltage-dependent current whose time constant is considerably faster than the duration of the delay.

Also important are the calcium-dependent potassium currents, collectively referred to as $I_{K(Ca)}$. Calcium ions that move into the cell during the depolarizing phase of the spike turn on these hyperpolarizing outward currents, rendering subsequent spiking that much more difficult. That this might have profound significance for the nervous system can be observed in hippocampus, neocortex, and elsewhere. The release of noradrenaline by brainstem fibers abolishes spike frequency accommodation, greatly increasing the excitability of these cells. Interestingly, the effect of blocking only I_{AHP} appears to be specific to increasing the slope of the cell's f–I curve, that is, increasing its gain.

We keep on drawing analogies between the operations the nervous system carries out to process information and digital computers. There are, of course, very deep, conceptual differences between the two. One is the amazing diversity seen in biology. An I_A current in a neocortical pyramidal cell is not the same as the I_A current in hippocampal pyramid cells or in thalamic relay cells. Each has its own unique activation and inactivation range, kinetics, and pharmacology, optimized by evolution for its particular role in the survival of the organism. A case in point appears to be calcium channels. So far, molecular biological techniques have revealed about a dozen different genes coding for two of the five subunits of the calcium channel, a number that is likely to increase over time. This provides the nervous system with the wherewithal to generate a very large number of calcium channels with different functional properties (Hofmann, Biel, and Flockerzi, 1994). This tremendous diversity could be necessary to allow each organism to optimize its complement of ionic currents for its particular operations depending on its particular and unique developmental history. This is, indeed, very far removed from the way we design and build digital integrated circuits using a very small library of canonical circuit elements.